



# Experimental study of a tuned mass damper endowed with changeable stiffness and eddy currents damping

Stefania Lo Feudo, Anissa Allani, Gwendal Cumunel, Pierre Argoul,  
Domenico Bruno

## ► To cite this version:

Stefania Lo Feudo, Anissa Allani, Gwendal Cumunel, Pierre Argoul, Domenico Bruno. Experimental study of a tuned mass damper endowed with changeable stiffness and eddy currents damping. 9ème Colloque National de l'Association Française du Génie Parasismique (AFPS) , Nov 2015, Marne-la-Vallée, France. hal-01424493

**HAL Id: hal-01424493**

**<https://hal.science/hal-01424493>**

Submitted on 2 Jan 2017

**HAL** is a multi-disciplinary open access archive for the deposit and dissemination of scientific research documents, whether they are published or not. The documents may come from teaching and research institutions in France or abroad, or from public or private research centers.

L'archive ouverte pluridisciplinaire **HAL**, est destinée au dépôt et à la diffusion de documents scientifiques de niveau recherche, publiés ou non, émanant des établissements d'enseignement et de recherche français ou étrangers, des laboratoires publics ou privés.

Copyright

# Etude expérimentale d'un amortisseur à masse accordée avec une raideur et un amortissement par courants de Foucault variables

## Experimental study of a tuned mass damper endowed with changeable stiffness and eddy currents damping

Stefania Lo Feudo\*,\*\* — Anissa Allani\* — Gwendal Cumunel\* — Pierre Argoul\* — Domenico Bruno\*\*

\* Laboratoire Navier, Université Paris-Est, UMR 8205 CNRS-ENPC-IFSTTAR

École des Ponts ParisTech, 6-8 Avenue Blaise Pascal, 77455 Marne-la-Vallée, France

{anissa.allani, gwendal.cumunel, pierre.argoul}@enpc.fr

\*\* DINCI, Università della Calabria

Via Pietro Bucci, 87036 Arcavacata, Rende CS, Italie

{stefania.lofeudo, d.bruno}@unical.it

**RÉSUMÉ.** Un Amortisseur à Masse Accordée (AMA) est un système de contrôle passif, consistant à attacher à une structure, un oscillateur linéaire dont la fréquence naturelle est synchronisée avec celle du mode à amortir. Cet article s'intéresse à la conception et à l'étude d'un AMA expérimental avec des coefficients d'amortissement et de raideur facilement réglables. Ainsi, l'amortissement de l'AMA est dû à un aimant placé au-dessus d'une masse en matériau conducteur, générant des courants de Foucault. La première étape de cette recherche est de vérifier si les paramètres modaux de l'AMA ainsi réalisé restent constants durant l'essai. Ainsi, pour différents réglages de l'AMA, ses paramètres modaux instantanés sont évalués à l'aide d'une procédure d'identification modale fondée sur la transformée en ondelettes continue des signaux mesurés. L'AMA est ensuite placé sur une maquette d'un bâtiment de trois étages et ses paramètres sont réglés sur ceux obtenus par optimisation d'un critère fondé sur le coefficient d'amplification dynamique. La réponse du portique avec et sans AMA, suite à un choc appliqué au dernier étage, est alors évaluée expérimentalement. Enfin le cas du portique avec ou sans AMA, soumis à une excitation sismique à sa base est modélisé et analysé numériquement.

**ABSTRACT.** The Tuned Mass Damper (TMD) is a structural passive control device attached on a structure and made by a linear oscillator which natural frequency is tuned to that of the structure, or to the dominant eigenfrequency. In this study, an experimental TMD with adjustable stiffness and damping is proposed. In particular, the TMD damping arises from the eddy current damping effect due to the presence of a permanent magnet placed on the top side of the TMD mass, which is made of conductive material. The first step is to check if the dynamical properties of the proposed TMD are constant during the dynamic test and for different values of stiffness and damping. Therefore, the instantaneous modal parameters are evaluated by applying the continuous wavelet transform on the experimental data. Then, the TMD is set with optimal parameters and used to control vibrations of a frame scale model. The structure response with and without the TMD is evaluated from the experimental measurements in case of shock at the top floor, and a numerical analysis is conducted in case of seismic ground acceleration.

**MOTS-CLÉS :** AMA, courants de Foucault, transformée en ondelettes continue, control passif.

**KEYWORDS:** TMD, eddy currents, continuous wavelet transform, passive control

### 1. Introduction

The Tuned Mass Damper (TMD) is a passive control device in which a mass-spring-dashpot system is attached to a primary structure, for example a tall building or a bridge (see (Soong et al., 1997) for a list of actual

applications). If the TMD is properly designed and properly tuned with the primary structure, it is able to reduce vibrations induced by external sources. Indeed, since an amount of vibration energy is transferred from the principal structure to the TMD, a dissipation energy mechanism is activated and the durability and the structural safety of the main structure can be greatly improved. Several criteria may be adopted in order to properly choose the TMD parameters. Among these, a class of optimization criteria is aimed to reduce the vibration energy of the system, which is referred as  $H_2$  norm optimization (Asami et al., 2001). Others strategies are based on the minimization of the transfer function maximum (Nishihara et al., 2002), and on the system poles location (Fujino et al., 1993). In addition, in the past decades several studies were conducted for different types of external excitation, especially concerning seismic loading. Indeed, a debate exists on the effectiveness of the damper masses and important studies were those carried out by (Sadek et al., 1997) and (Rana et al., 1998). Also (Hadi et al., 1998) applied the  $H_\infty$  norm optimization to a MDoF structure endowed with a TMD. The authors found that for the case studied the control device was effective in reducing the vibration response, even though at the beginning of the excitation the response of the structure appeared quite similar to the uncontrolled case. Then, (Lee et al., 2006) analyzed the MDoF structure response with a single or multiples TMDs and (Bekdaç et al., 2011) proposed a new procedure, called Harmonic Search, in which the parameter are obtained for a harmonic load, and then checked in case of earthquake. They obtained a considerable reduction in the maximum top story displacement, and remarked that optimal parameters are numerically small, which may be preferable since forces acting on the building from TMD are less, and owing to a likely cost reduction.

In this research study, the effectiveness of an experimental TMD model proposed by the authors in (Lo Feudo et al., 2015) is further investigated. In particular, the TMD is used to control vibration of a three stories frame scale model, and placed on its top floor. The TMD, which mass is fixed for practical issues, has adjustable stiffness and damping coefficient, in order to allow the investigation of the proposed experimental model and to easily set the TMD with optimal parameters. The damping of the TMD is due to the eddy currents damping effect, which arises when a non-magnetic conductive material is subjected to a time-varying magnetic field (Graves et al., 2000). Indeed, induced currents appear into the conductor and circulate in such a way to generate a magnetic field, which opposes the original change in magnetic flux. In addition, a Lorentz force contrasts the motion and, owing to the resistance of the conductor, energy is dissipated into heat and a vibrations reduction is achieved. This mechanism is adopted in several fields, such as in braking systems, vibration control of rotating systems, vibration isolation in levitation systems and also for the structural vibration suppression (Sodano et al., 2004). One of the major advantages of adopting this damping mechanism is the lack of contact between the eddy current damper and the system to damp. Indeed, the material properties are unaffected by its addition, and the performance does not degrade over the time. For example, in order to control vibration of a beam, an eddy currents damper was analyzed by (Bae et al., 2012) and (Wang et al., 2012), and also was recently used by the Gensler Architecture firm as a passive control device for the Shanghai Tower, which is 623 m tall. The TMD is placed on the 125th floor, it occupies five floors and it weighs about 1,000 tons. In particular, the TMD is made by 1,076-square-foot copper plate covered with 125 powerful magnets, mounted beneath a suspended mass damper, consequently such a system, according to the designers, is able to resist a 2500-year earthquake (Gao et al., 2014).

The present work is organized as follows. In the first sections, the TMD governing equations are briefly presented, together with the eddy current damping effect principle. Next, the proposed experimental TMD is described. Then, the TMD is tested and used in order to control vibrations of a frame scale model. In particular, the TMD is optimized starting from experimental results when a shock is applied on the structure top floor, and by using a numerical model in case of ground motion acceleration. Some remarks conclude the paper.

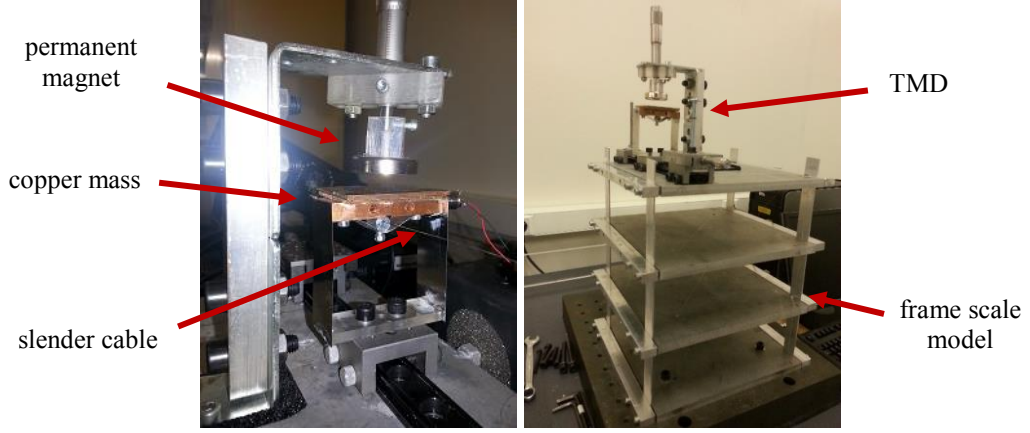


**Figure 1.** Experimental eddy currents Tuned Mass Damper

## 2. TMD governing equations

Let's consider the system represented in Figure 1, where a TMD is located on the top floor of a NDoF structure, where the floors may be considered as infinitely stiff and the masses as concentrated at the floor levels. Therefore,  $\mathbf{M}_s$ ,  $\mathbf{C}_s$  and  $\mathbf{K}_s$  are the mass, damping and stiffness matrices of the NDoF system,  $\mathbf{F}(t)$  is the vector of external forces,  $\mathbf{F}_T(t)$  the force exerted on the structure by the TMD, and  $\mathbf{M}_s \mathbf{I} \ddot{u}_g(t)$  the earthquake base acceleration, where  $\mathbf{I}$  is the unit vector. With the aim to control the predominant  $i$ -mode and the relative displacement with respect to the ground of the  $n$ -th floor,  $u_n$ , the equations of motion may be expressed in the following form:

$$\begin{aligned} m_{si,n}^* \ddot{u}_n(t) + c_{si,n}^* \dot{u}_n(t) + k_{si,n}^* u_n(t) &= f_{i,n}^*(t) + f_{Ti,n}^*(t) - m_{si,n}^* \Gamma_{i,n}^* \ddot{u}_g(t), \quad i=1, \dots, n \\ m_T (\ddot{u}_T(t) + \ddot{u}_g(t)) + c_T (\dot{u}_T(t) - \dot{u}_n(t)) + k_T (u_T(t) - u_n(t)) &= 0 \end{aligned} \quad [1]$$

where  $m_T$ ,  $c_T$  and  $k_T$  are the TMD mass, damping coefficient and stiffness, respectively,  $u_T$  is the TMD relative displacement, and

$$\begin{aligned} \mathbf{m}_s &= \Phi^T \mathbf{M}_s \Phi, \quad \mathbf{c}_s = \Phi^T \mathbf{C}_s \Phi, \quad \mathbf{k}_s = \Phi^T \mathbf{K}_s \Phi, \quad \mathbf{f}(t) = \Phi^T \mathbf{F}(t), \quad \mathbf{f}_T(t) = \Phi^T \mathbf{F}_T(t), \quad \mathbf{g} = \Phi^T \mathbf{M}_s \mathbf{I}, \\ m_{si,n}^* &= \frac{m_{si}}{\Phi_{in}^2}, \quad c_{si,n}^* = \frac{c_{si}}{\Phi_{in}^2}, \quad k_{si,n}^* = \frac{k_{si}}{\Phi_{in}^2}, \quad f_{i,n}^*(t) = \frac{f_i(t)}{\Phi_{in}}, \quad f_{Ti,n}^*(t) = \frac{f_{Ti}(t)}{\Phi_{in}}, \quad \Gamma_{i,n}^* = \frac{g_i}{\Phi_{in} m_{si,n}^*} \end{aligned} \quad [2]$$

wherein  $\Gamma_{i,n}^*$  denotes the modal participation factor, and  $\Phi$  is the modal matrix, which can be evaluated by solving the generalized eigenproblem  $\mathbf{K}_s \Phi_i = \omega_{si}^2 \mathbf{M}_s \Phi_i$ , where  $\omega_{si}$  are the modal frequencies. By passing to the frequency domain, and by applying the Fourier transform, it is also possible to define the dynamic stiffness matrix,  $\mathbf{G}^*(\omega)$  as follows:

$$\mathbf{G}^*(\omega) = \begin{bmatrix} -\omega^2 m_{si,n}^* + i\omega c_{si,n}^* + k_{si,n}^* + i\omega c_T + k_T & -(i\omega c_T + k_T) \\ -(i\omega c_T + k_T) & -\omega^2 m_T + i\omega c_T + k_T \end{bmatrix} \quad [3]$$

which enables to pass from a set of differential equations, [1], to a set of algebraic equations through  $\mathbf{G}^*(\omega) \mathbf{u}(\omega) = \mathbf{P}(\omega)$ , where

$$\begin{aligned} \mathbf{u}(\omega) &= [u_n(\omega), u_T(\omega)]^T \\ \mathbf{P}(\omega) &= [f_{i,n}^*(\omega) - m_{si,n}^* \Gamma_{in}^* \ddot{u}_g(\omega), -m_T \ddot{u}_g(\omega)]^T \end{aligned} \quad [4]$$

Finally, it is possible to introduce the normalized dynamic flexibility matrix, which can be evaluated as:

$$\mathbf{H}^*(\omega) = \mathbf{G}^{*-I}(\omega) \quad [5]$$

### 2.1. Optimization criterion

The TMD's performance, sensibility and robustness depend highly by its dynamical properties. Therefore, with the aim to properly set the TMD parameters, several optimization criteria were proposed in a large number of previous studies. In fact, the criterion to adopt is one of the most important design decisions, which may depend by several factors, as the nature of the external excitation, the type of structure, the technical and economic feasibility, etc. In particular, in this study, the chosen optimization criterion belongs to a class of criteria aimed to reduce the vibrational energy of the system. Indeed, such an approach was proved to be quite effective and robust, (Allani, 2015), and in general it leads to lower damping ratio values, which are preferable from a practical point of view. Therefore, the optimization criterion consists in minimizing a cost function which depends on the frequency response function (FRF) of the n-th floor, which is the floor to be controlled. In particular, the objective is to minimize the ratio between the square root of the squared absolute value of the FRF in the controlled case and in the uncontrolled case, i.e. when no TMD is used. Moreover, the above quantities are evaluated within a frequency range of interest,  $[\omega_1, \omega_2]$ , where  $\omega_1$  and  $\omega_2$  are the lower and upper frequency bound considered, respectively. According to (Allani, 2015), the criterion may be set in the following form:

$$C_f(k_T, c_T) = \frac{\sqrt{\int_{\omega_1}^{\omega_2} \left| \frac{u_n(\omega)}{F_n(\omega)} \right|^2 d\omega}}{\sqrt{\int_{\omega_1}^{\omega_2} \left| \frac{u_{n0}(\omega)}{F_n(\omega)} \right|^2 d\omega}}, \quad C_e(k_T, c_T) = \frac{\sqrt{\int_{\omega_1}^{\omega_2} \left| \frac{u_n(\omega)}{\ddot{u}_g(\omega)} \right|^2 d\omega}}{\sqrt{\int_{\omega_1}^{\omega_2} \left| \frac{u_{n0}(\omega)}{\ddot{u}_g(\omega)} \right|^2 d\omega}} \quad [6]$$

where  $|u_n(\omega)/F_n(\omega)|$  and  $|u_n(\omega)/\ddot{u}_g(\omega)|$  are the moduli of the FRF referred to the cases of force acting on the top floor and ground acceleration, respectively, and  $|u_{n0}(\omega)/F_n(\omega)|$  and  $|u_{n0}(\omega)/\ddot{u}_g(\omega)|$  denote the same quantities of above, but evaluated when no TMD is placed on the structure. Therefore, for an uncontrolled structure, the criterion was setting up in such a way that it is equal to one. Hence, by keeping fixed for practical issues the TMD mass,  $m_T$ , the design parameters to be chosen are the TMD stiffness and damping coefficient,  $k_T$  and  $c_T$ , respectively, which minimize the above cost functions.

### 3. Eddy currents damping effect

In this section, the governing equations related to eddy currents will be briefly recalled, according to the formulation used in (Bae et al., 2012) and reported by (Lo Feudo et al., 2015). When a conductive material moves through a stationary magnetic field, since it is subjected to a time-varying magnetic field, eddy currents are induced. By neglecting the surface charge in the conductive plate, the eddy currents density is given by

$$\mathbf{J} = \sigma(\mathbf{v} \times \mathbf{B}) \quad [7]$$

where  $\sigma$  is the material electrical conductivity,  $\mathbf{v}$  is the relative velocity between the permanent magnet and the conductor,  $\mathbf{B}$  is the magnetic flux density and  $\mathbf{v} \times \mathbf{B}$  represents the electromotive force driving the eddy currents. Since the eddy currents generate another magnetic field, which polarity is opposite to those due to the

permanent magnet, a repulsive force appears. This force can be evaluated according to the Lorentz's Law and, if the velocity has a component only in the x direction, it takes the following form:

$$\mathbf{F} = \int_V (\mathbf{J} \times \mathbf{B}) dV = \sigma v_x \int_V [(-B_z^2 - B_y^2) \mathbf{i} + B_x B_y \mathbf{j} + B_x B_z \mathbf{k}] dV \quad [8]$$

where V is the conductor volume. Hence, according also to (Wang et al., 2012), the electromagnetic force evaluated in the x direction does not depend on the  $B_x$  component of the magnetic field. Therefore, the damping force in the x direction is proportional to the velocity vector with opposite direction, and a linear damping coefficient of the TMD may be defined as follows:

$$c_T = \sigma \int_V (B_y^2 + B_z^2) dV \quad [9]$$

#### 4. Experimental TMD

The proposed experimental TMD is made of a 0.15 kg copper mass, which is supported by two thin steel sheets. The device is designed in such a way to allow a manual adjustment of the natural frequency and of the inherent damping, and is placed on the top floor of a building scale model (Figure 1). The bottom of the mass is also connected to a slender cable fixed at the two ends. One of the cable's support position is adjustable, so that the amount of stretch in the slender cable can be manually adjusted. As long as the cable tensile stress is increased, the TMD stiffness and natural frequency rise. In this study, by considering the frequency bandwidth of interest, the support is moved over a range of 0.4 mm with a step size of 0.04 mm. The damping of the TMD is conversely given by a magnet located up to the mass. Indeed, since the conductive mass is subjected to a time-varying magnetic field, eddy currents are induced in the conductor. The distance between the magnet and the mass is adjustable, and the gap is moved from 3.35 mm to 5.35 mm, with a step size of 0.2 mm.

The evaluation of the TMD frequency and damping ratio is carried out by applying on experimental data the Continuous Wavelet Transform (CWT), which enables to estimate the instantaneous value of modal frequencies, damping and mode shapes. In particular, the CWT of an asymptotic signal is concentrated along some curves in the time-frequency domain called ridges, and the restriction of the CWT to each ridge is called skeleton of the wavelet. The skeleton gives the natural frequency of the signal, whereas the time evolution of the logarithm of the Wavelet transform amplitude gives information about damping, for further explanation please see (Le et al., 2004). Therefore, in order to characterize the TMD properties behavior also when the magnet distance and the stretch in the cable are changed, the response of the TMD alone was recorded in several free vibration tests. For each fixed value of tensile cable stress, the temporal response of the TMD was measured by changing the gap between the magnet and the mass, by carrying out each test three times. Then, the CWT was applied on data, which results were already presented in (Lo Feudo et al., 2015) and will be here briefly reported. In Figure 2, the instantaneous values of TMD frequency and damping ratio, and the force - displacement trend are shown for a chosen TMD configuration. By looking within the domain of interest, which is delimited by the solid red thick lines (Le et al., 2004), it emerges that the frequency keeps almost constant during the test, whereas the damping ratio exhibits a non-linear behavior. However, this non-linearity seems to depend mostly on the intensity of the excitation (shock), than on the distance between the magnet and the mass. However, from Figure 2 it appears also that the damping force-displacement plot has a comparable behavior with respect to those of a linear oscillator. In Figure 3, results obtained in terms of modal parameters by changing the TMD configuration are summarized. In particular, the damped frequency and the damping ratio reported are the average values taken over the time interval for each test, and over the number of test (3) performed for each configuration. As a result, for a fixed tension in the cable, the frequency keeps constant by varying the distance of the magnet, and it varies linearly by displacing the cable support. Conversely, the damping ratio has nearly a nonlinear behavior with respect to the magnet position and the cable tensile stress.

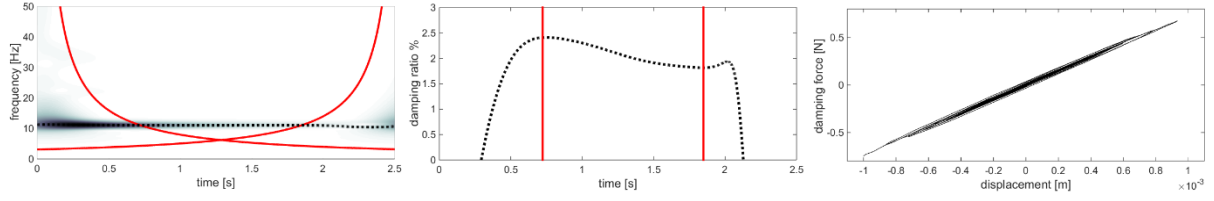


**Figure 2.** From left to right: CWT, damping ratio and damping force – displacement behavior of the TMD under an impulsive shock when the gap between magnet and copper mass is equal to 4,35 mm

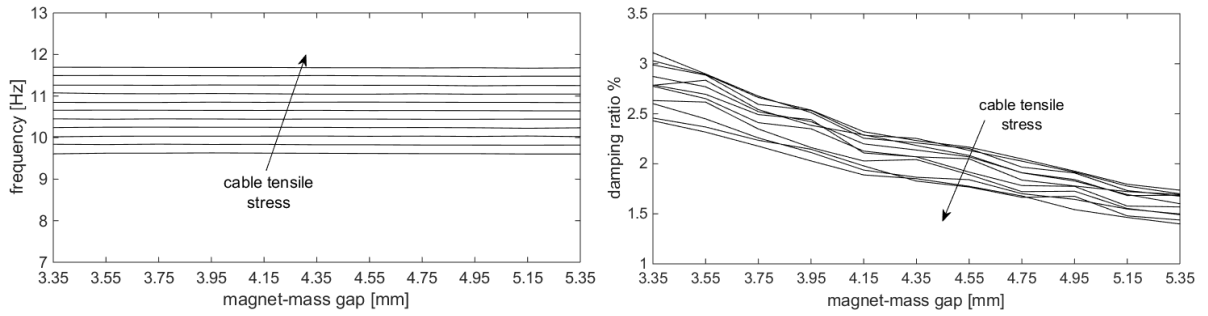


**Figure 3.** TMD's properties by varying the cable stretching and the gap between magnet and copper mass

## 5. Applications for vibration control of a frame scale model

The TMD is placed on the top of a three stories frame structure, which horizontal planes are made by aluminum plates supported by four thin aluminum beams placed on two opposite sides of the plates. The floors weights are  $m_1 = 2.43$  kg,  $m_2 = 2.43$  kg and  $m_3 = 3.76$  kg, where the subscript 1 denotes the lower floor. In particular, the top floor hosts two fixed supports for the TMD, which allow to change its stiffness and damping and which are considered as a part of the principal structure. The instantaneous modal properties of the structural system, without the TMD, are evaluated by applying the CWT on the experimental signals obtained after an impact on the top floor. However, in order to implement a numerical model, the stiffness and the damping coefficient have to be evaluated. In this study, the Modal Assurance Criterion (MAC) is adopted, that is a model updating method able to measure the consistency, namely the degree of linearity, between two different modal vectors (Allemang, 2003). In particular, the experimental results are considered as the reference model, whereas the numerical results are obtained by iteration starting from the identification parameters, which are the unknowns of the problem, i.e. the stiffness and the damping coefficients. The MAC is bounded between zero and one, with zero representing no consistent correspondence. Therefore, for each set of unknowns, the mode shapes are evaluated and an objective function is minimized. In the standard formulation, the latter is defined as the relative error between modal frequencies and mode shapes obtained from a set of unknowns parameters ( $f_{num,i}$ ,  $\phi_{num,i}$ ) in the numerical case and in the reference solution ( $f_{exp,i}$ ,  $\phi_{exp,i}$ ), (Gambarelli et al., 2015). In order to equally take into account the correspondence between the frequencies and the mode shapes, the objective function to minimize is defined according to (Gentile, 2007) as:

$$J_{obj} = \frac{1}{n} \sum_{i=1}^n \left[ \left| \frac{(f_{exp,i} - f_{num,i})}{f_{exp,i}} \right| + NMD_i \right] \quad [10]$$

where  $NMD_i = \sqrt{(1 - MAC)/MAC}$  is the Normalized Modal Difference, which is adopted in order to estimate the average difference between two modal vectors, (Mardini et al., 2007); a NMD value close to zero denotes a better correlation. The comparison between experimental and numerical results in term of modal frequencies, and mode shapes through the MAC and the NMD is reported in Table 1. A high correlation is found for the first mode, although the error slightly increases for the other two modes. A good correspondence exists in the structural response after a shock, as shown in Figure 4. In particular, the experimental signals are filtered in order to eliminate an unwanted low frequency component and a frequency component arising from the fixed support of the TMD. Indeed, since their mass is small with respect to the floor mass, they are supposed to be part of the top floor.

mode	experimental frequency [Hz]	numerical frequency [Hz]	Error %	MAC %	NMD
1	10.7704	10.7705	2.5216E-04	99.9768	0.0152
2	30.7199	31.8445	3.7910E+00	99.9256	0.0273
3	48.3850	48.0428	-7.0730E-01	98.8315	0.1087

**Table 1.** Model updating method results

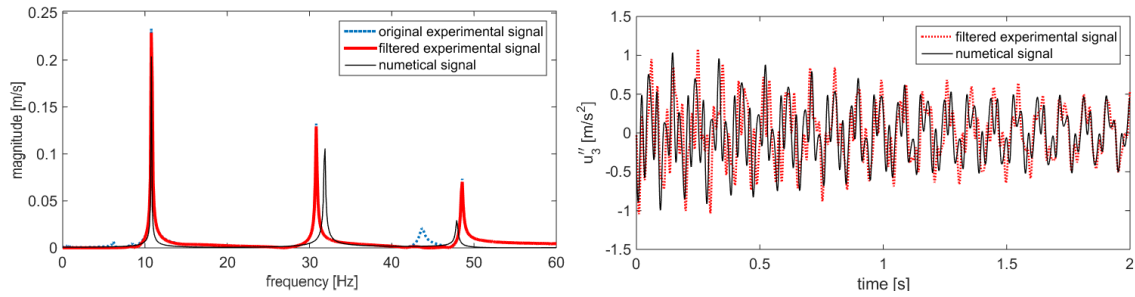


**Figure 4.** Experimental and numerical top floor response

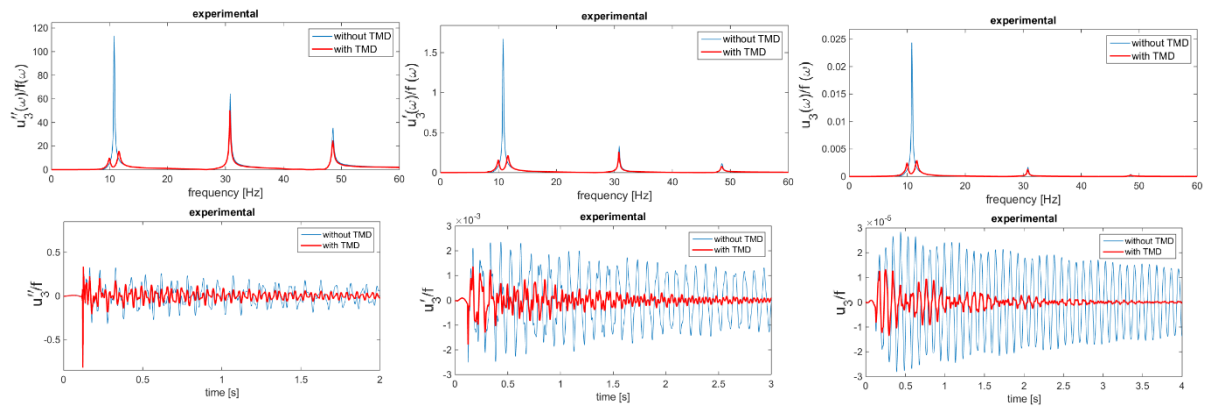


**Figure 5.** Structural response of the scale model top floor in the uncontrolled case and when a TMD is used with optimal parameters, namely  $f_T = 11.04$  Hz and  $\xi_T = 2.04\%$



### 5.1. Free vibrations

The frame scale model free vibrations are recorded and analyzed when an impact force is applied on the top floor of the frame scale model. Then, the structural response is compared when no control device is used at all, and when the TMD is attached on the structure and set with optimal parameters. In particular, the optimal values of TMD frequency and damping are chosen by evaluating, for each combination of TMD properties here considered, the function  $C_F$  reported in Eq. [6]. The combinations of damped frequency and damping ratio ( $f_T, \xi_T$ ) which corresponds to a minimum for  $C_F$  is selected as the optimum configuration. However, this is not a numerical procedure, but an experimental optimization conducted among a limited range of dynamical properties, namely  $f_T = 9.6 \div 11.7$  Hz and  $\xi_T = 1.40 \div 3.11$  %. In Figure 5, the FRFs and the top floor response are reported in the uncontrolled and in the controlled cases. The TMD greatly reduces the first peak of the FRFs, which is also split into two. Moreover, although the TMD is tuned with only the first modal frequency and it does not affect greatly the others, a global response reduction may be observed in term of acceleration, velocity and roof displacement.

### 5.2. Numerical analysis under ground motion acceleration

The effectiveness of the proposed TMD is here numerically evaluated when the structure is subjected to a ground motion acceleration. To this end, three recorded accelerograms (El Centro NS 1940, L'Aquila AQV – EW 2009 and Friuli GMN – EW 1976), and an artificial one were chosen and scaled in such a way that the first modal frequency of the uncontrolled structure falls in the earthquake frequency content, as shown in Figure 6. The value assumed by the cost function  $C_E$  presented in Eq. [6], which is valid under ground motion acceleration, is shown in Figure 7 for different TMD properties. As it could be seen, for each combinations of TMD properties, a structural response reduction in term of energy is obtained since  $C_E$  always keeps less than 1. An optimal combination of damping ratio and stiffness of the added mass can also be identified. In particular, as expected, the optimal TMD frequency value is in the neighborhood of the scale model first modal frequency, although it slightly varies with the accelerogram considered. In Figure 8, the response of the controlled and uncontrolled structure is compared when the TMD is set with the optimal parameters. As it could be seen, in the first instant of the earthquake, the top floor displacement is not influenced by the presence of the TMD. On the contrary, in the next part a high response reduction may be observed since a larger amount of energy can be transferred from the structure to the TMD.

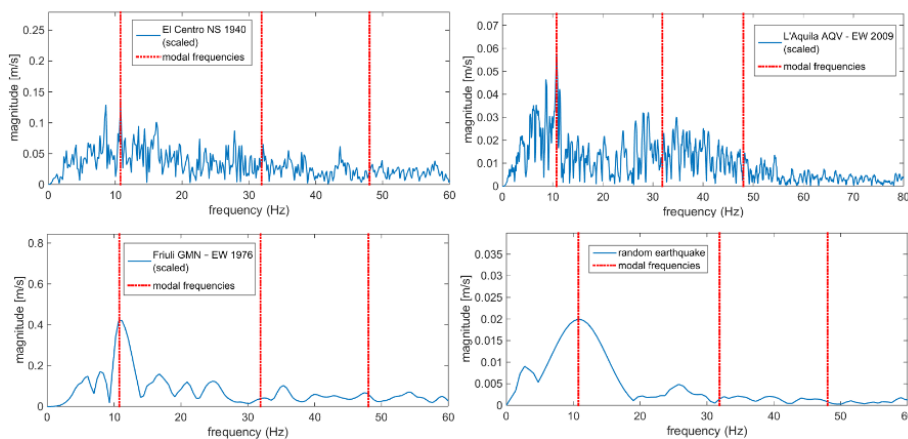


**Figure 6.** Frequency content of the scaled accelerograms and frame scale model modal frequencies

## 6. Conclusion

In this study, an experimental TMD endowed with adjustable stiffness and damping, and based on the eddy currents damping effect, is studied. The CWT is applied on the experimental free vibration signals of the proposed TMD. As a result, it is obtained that the TMD frequency keeps constant during the dynamic test, whereas the damping ratio behaves non-linearly in the first instants. Moreover, the TMD frequency increases linearly with the cable tensile stress, whereas the damping ratio varies non-linearly by varying the gap between a circular magnet and the damper mass. The TMD is then attached on the top floor of a three stories frame scale model. Optimal parameters are found in order to control the structure under impulsive shock, and the TMD is shown to be very effective. Finally, a numerical analysis is conducted in case of ground motion acceleration. It appears that, if the earthquake frequency content matches the structure mode for which the TMD is tuned, a response reduction may be observed. However, the TMD optimal parameters depend on the considered accelerogram, so that a statistical analysis of strong-motion accelerograms may be required.

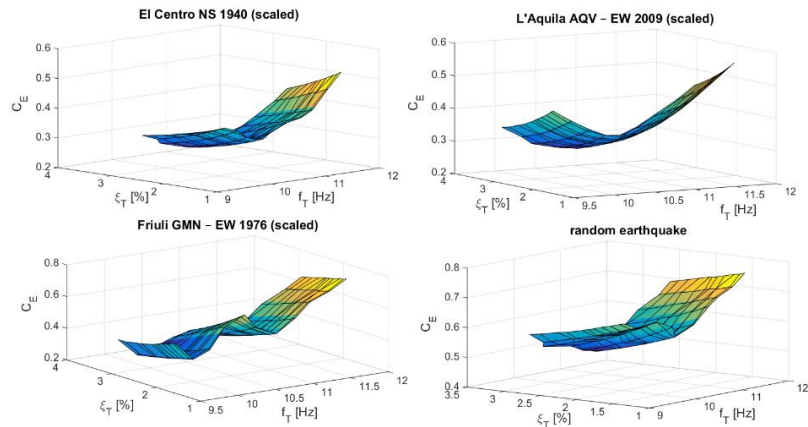


**Figure 7.** Numerical variation of the optimization criterion depending on the TMD configuration

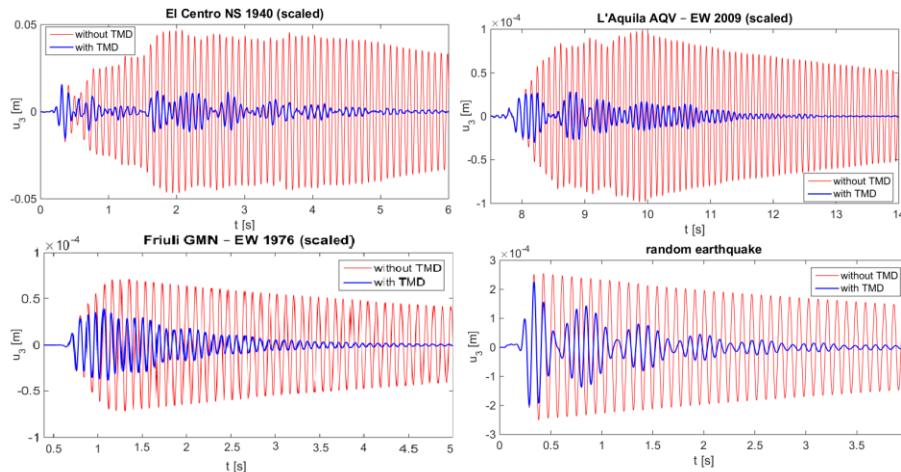


**Figure 8.** Numerical top floor displacement when the optimum values for the TMD are used, which properties are:  $f_T = 10.44$  Hz,  $\xi_T = 2.84\%$  for El Centro NS 1940;  $f_T = 10.44$  Hz,  $\xi_T = 2.84\%$  for L'Aquila AQV - EW 2009;  $f_T = 10.02$  Hz,  $\xi_T = 3.11\%$  for Friuli GMN - EW 1976 and  $f_T = 10.66$  Hz,  $\xi_T = 2.79\%$  for the random earthquake.

## 7. References

- Allani A., Amortissement multimodal dans les grandes structures souples en vibration, Unpublished PhD Thesis, Université Paris-Est & Università di Roma "Tor Vergata", 2015.
- Allemang R. J., "The modal assurance criterion-twenty years of use and abuse," *Sound and Vibration*, 2003, p. 14-21.
- Asami, T, Nishihara O., Baz A. M., "Closed-form exact solution to  $H_2$  optimization of dynamic vibration absorber attached to damper linear systems," *Transactions of the Japan Society of Mechanical Engineers*, vol. 67, n° 655, 2001, p. 597-603.
- Bae J., Hwang J., et al, "Vibration suppression of a cantilever beam using magnetically tuned-mass-damper," *Journal of Sound and Vibration*, vol. 331, 2012, p. 5669-5684.
- Bekdaç G., Nigdeli S. M., "Estimating optimum parameters of tuned mass dampers using harmony search," *Engineering Structures*, vol. 33, 2011, p. 2716-2723.
- Fujino Y., Abe, M., "Design formulas for tuned mass dampers based on a perturbation technique," *Earthquake Engineering and structural dynamics*, vol. 22, n° 10, 1993, p. 833-854.
- Gambarelli P., Vincenzi L., *A surrogate-assisted evolutionary algorithm for dynamic structural identification*, Engineering Optimization IV, CRC press, 2015.
- Gao Z., Shi D., "Construction Technology and Management Innovation," *Council on Tall Buildings and Urban Habitat*, 2014, p. 103-111
- Gentile C., "Operational modal analysis of curved cable-stayed bridges," *2nd Int. Operational Modal Analysis Conf. (IOMAC'07)*, 30 April – 2 May 2007, Copenhagen, p. 75-86.
- Graves K. E., Toncich D., Iovenitti P. G., "Theoretical comparison of motional and transformer EMF device damping efficiency," *Journal of Sound and Vibration*, vol. 233, n° 3, 2000, p. 441-453.
- Hadi M. N., Arfiadi Y., "Optimum Design of Absorber for MDOF Structures," *Journal of Structural Engineering*, vol. 124, n° 11, 1998, p. 1272-1280.
- Le T., Argoul P., "Continuous wavelet transform for modal identification using free decay response," *Journal of Sound and Vibration*, vol. 277, n° 3, 2004, p. 73-100.
- Lee C., Chen Y., "Optimal design theories and applications of tuned mass dampers," *Engineering Structures*, vol. 28, 2006, p. 43-53.
- Lo Feudo S., Allani A., et al., "Experimental Tuned Mass Damper Based on Eddy Currents Damping Effect and Adjustable Stiffness," *CSMA 2015, 12 Colloque National en Calcul des Structures*, 18-22 May 2015, Giens, France.
- Mordini A., Savov K., "The Finite Element Model Updating: A Powerful Tool for Structural Health Monitoring," *Structural Engineering International*, vol. 17, n° 4, 2007, p. 352-358.
- Nishihara O., Asami T., "Closed-Form Solutions to the Exact Optimizations of Dynamic Vibration Absorbers (Minimizations of the Maximum Amplitude Magnification Factors)," *Journal of Sound and Vibration*, vol. 124, n° 4, 2002, p. 576-582.
- Rana R., Soont T. T., "Parametric study and simplified design of tuned mass dampers," *Engineering Structures*, vol. 20, n° 3, 1998, p. 193-204.
- Sadek F., Mohraz B., et al., "A method of estimating the parameters of tuned mass dampers for seismic applications," *Earthquake Engineering and Structural Dynamics*, vol. 26, 1997, p. 617-635.
- Sodano H. A., Bae J., "Eddy Current Damping in Structures," *The Shock and Vibration Digest*, vol. 36, 2004, p. 469-478.
- Soong T. T., Dargush G. F., *Passive Energy Dissipation Systems in Structural Engineering*, Wiley: New York, 1997.
- Wang Z., Chen Z., Wang J., "Feasibility study of a large-scale tuned mass damper with eddy current damping mechanism," *Earthquake Engineering and Engineering Vibration*, vol. 11, n° 3, 2012, p. 391-401.